J. Mater. Environ. Sci. 6 (8) (2015) 2301-2314
ISSN : 2028-2508
CODEN: JMESCN

Theoretical prediction and experimental study of 2-phenyl-1, 4-dihydroquinoxaline as a novel corrosion inhibitor for carbon steel in 1.0 HCl

F. Benhiba[a], H. Zarrok[a], A. Elmidaoui[a], M, El Hezzat[e], R. Touir[f,g], A. Guenbour[b], A. Zarrouk[c], S. Boukhris[d] , H. Oudda[a,*]

[a] *Laboratory of Separation Processes, Central Post, Kenitra , Department of Chemistry, Faculty of Sciences, University Ibn Tofail, Morocco.*
[b] *Laboratory of Nanotechnology, Materials, and the Environment Faculty of Sciences, Rabat, Morocco*
[c] *LCAE-URAC18, Faculté des Sciences, Université Mohammed I[er] B.P. 717, M-60000 Oujda, Morocco*
[d] *Laboratory of Organic Synthesis, Organometallic and theoretical, Faculty of Sciences, University Ibn Tofail, Kenitra, Morocco.*
[e] *Laboratoire de Physico-Chimie du Solide (LPCS), Faculté des Sciences, Université Ibn Tofail, Kenitra, Morocco.*
[f] *Laboratoire des Matériaux, Electrochimie et Environnement, Faculté des Sciences, Université Ibn Tofail, BP 133, Kénitra 14000, Morocco.*
[g] *Centre Régional des métiers de l'éducation et de la formation (CRMEF), Madinat Al Irfane, BP 6210 Rabat, Morocco.*

Received 24 Apr 2015, Revised 21 Jul 2015, Accepted 22 Jul 2015
**Corresponding author: E-mail: ouddahassan@gmail.com*

Abstract
Corrosion inhibition by 2-phenyl-1, 4-dihydroquinoxaline (PHQ) on carbon steel in 1.0 M HCl is investigated using electrochemical techniques (EIS and Potentiodynamic polarization), SEM and quantum chemical calculation. Inhibition efficiency of 89% is reached with 5×10^{-3} M of PHQ at 303 K. Potentiodynamic polarization showed that the PHQ behaves as mixed-type inhibitor. The Nyquist plots showed that increasing PHQ concentration, charge-transfer resistance increased and double-layer capacitance decreased, involving increased inhibition efficiency. Adsorption of the inhibitor molecules corresponds to Langmuir adsorption isotherm. Also, the activation thermodynamic parameters of dissolution were calculated and discussed. Theoretical calculations have been used to make the correlation between the effectiveness of inhibition of our studied inhibitor and their molecular structure.

Keywords: Carbon steel, HCl, Corrosion inhibition, Electrochemical techniques, Theoretical studies.

1. Introduction
Iron and its alloys play crucial roles in our daily lives due to their excellent properties, such as high structural and mechanical strengths [1,2]. These materials are used in various industrial and engineering applications. Acid-pickling, acid-cleaning, aciddescaling and oil-well acidizing are well-known industrial processes for cleaning the surfaces of metals. Acid solutions are used for these applications. It is necessary to use acid solutions to remove undesirable scale and corrosion products from metals. Hydrochloric acid and sulphuric acid are commonly used for this purpose; however, these acids attack the metal and initiate corrosion. This corrosion can cause serious damage to the metal and degrade its properties, thereby limiting its applications [3-6]. The use of inhibitors is the most important method for protecting metals from corrosion, and many scientists are conducting research on this topic. New inhibitors are discovered every day. In principle, inhibitors prevent the corrosion of metal by interacting with the metal surface via adsorption through the donor atoms, π-orbitals, electron density and the electronic structure of the molecule [7-25]. Inhibitor molecules are adsorbed onto the metal surface, thus resulting in film formation. The adsorbed film acts as a barrier, which separates the metal surface from the corrosive medium and consequently decreases the extent of corrosion. In general, the adsorption of inhibitor molecules on the metal surface depends on the nature and the surface charge of the metal, the adsorption mode, chemical structure and type of electrolyte solution.
The quinoxalines are the heterocycles that frequently found in compounds propertied diverse biological activities [26-29]. In addition, several studies have already carried on the corrosion inhibition of steel in acid medium with organic compounds of type of «quinoxalines» [30-37], have given very good results, which pushed us to seek other new derivatives for testing their inhibitory effects on carbon steel in 1.0 HCl medium.

Quantum chemical calculations are very effective methods for determining a correlation between molecular structure and inhibition efficiency. They can also be utilized to support the accuracy of experimental results [38-40]. Thus, it is important to compute the quantum chemical parameters, such as the energy of the highest occupied molecular orbital (E_{HOMO}), the energy of the lowest unoccupied molecular orbital (E_{LUMO}), the fraction of electrons transferred (ΔN) and the energies of the frontier molecular orbitals. In the present study, density functional theory (DFT) was used to determine the molecular structure of 2-phenyl-1, 4-dihydroquinoxaline (PHQ) as a corrosion inhibitor for CS.The corrosion inhibition behaviour of PHQ on the CS in acidic solution was investigated using electrochemical techniques and SEM. The chemical structure of the studied (PHQ) is given in Fig 1.

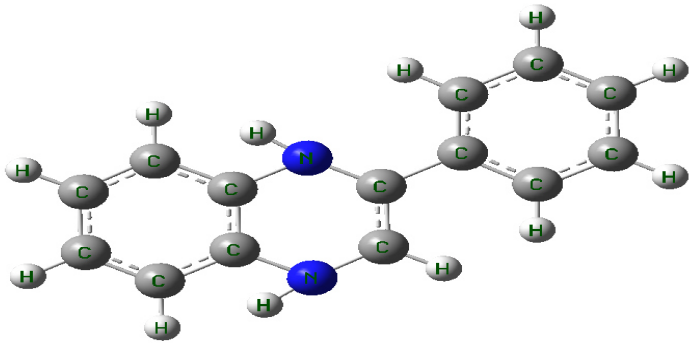

Figure1. The chemical structure of the studied 2-phenyl-1, 4-dihydroquinoxaline compound

2. Materials and methods

2.1. Materials

The steel used in this study is a carbon steel (CS) (carbon steel and US specification: SAE 1035) with a chemical composition (in wt%) of 0.370 % C, 0.230 % Si, 0.680 % Mn, 0.016 % S, 0.077 % Cr, 0.011 % Ti, 0.059 % Ni, 0.009 % Co, 0.160 % Cu and the remainder iron (Fe).

2.2. Solutions

The aggressive solutions of 1.0 M HCl were prepared by dilution of analytical grade 37% HCl with distilled water. The concentration range of 2-phenyl-1, 4-dihydroquinoxaline (PHQ) used was 1×10^{-5} M to 5×10^{-3} M.

3. Polarization measurements

3.1. Electrochemical impedance spectroscopy

The electrochemical measurements were carried out using a Volta lab (PGZ 100) potentiostate and controlled by (Voltamaster 4) at under static condition. The corrosion cell used had three electrodes. The reference electrode was a saturated calomel electrode (SCE). A platinum electrode was used as auxiliary electrode of surface area of 1 cm^2. The working electrode was carbon steel with the surface area of 1 cm^2. All potentials given in this study were referred to this reference electrode. The working electrode was immersed in test solution for 30 minutes to a establish steady state open circuit potential (Eocp). After measuring the Eocp, the electrochemical measurements were performed. All electrochemical tests have been performed in aerated solutions at 303 K. The EIS experiments were conducted in the frequency range with high limit of 100 kHz and different low limit 0.1 Hz at open circuit potential, with 10 points per decade, at the rest potential, after 30 min of acid immersion, by applying 10 mV ac voltage peak-to-peak. Nyquist plots were made from these experiments. The best semicircle can be fit through the data points in the Nyquist plot using a non-linear least square fit so as to give the intersections with the x-axis.

The inhibition efficiency of the inhibitor was calculated from the charge transfer resistance values using the following equation [41]:

$$\eta_z\,\% = \frac{R_{ct}^{i} - R_{ct}^{\circ}}{R_{ct}^{i}} \times 100 \qquad (1)$$

Where, R_{ct}° and R_{ct}^{i} are the charge transfer resistance in absence and in presence of inhibitor, respectively.

3.2. Potentiodynamic polarization

The electrochemical behaviour of carbon steel sample in inhibited and uninhibited solution was studied by recording anodic and cathodic potentiodynamic polarization curves. Measurements were performed in the 1.0 M HCl solution containing different concentrations of the tested inhibitor by changing the electrode potential automatically from -800 to 0 mV versus corrosion potential at a scan rate of 1 mV^{s-1}. The linear Tafel segments of anodic and cathodic curves

were extrapolated to corrosion potential to obtain corrosion current densities (I_{corr}). From the polarization curves obtained, the corrosion current (I_{corr}) was calculated by curve fitting using the equation:

$$I = I_{corr}\left[exp\left(\frac{2.3\Delta E}{\beta_a}\right) - exp\left(\frac{2.3\Delta E}{\beta_c}\right)\right] \quad (2)$$

The inhibition efficiency was evaluated from the measured I_{corr} values using the relationship:

$$\eta_{Tafel}\% = \frac{I^{\circ}_{corr} - I^{i}_{corr}}{I^{\circ}_{corr}} \times 100 \quad (3)$$

Where, I°_{corr} and I^{i}_{corr} are the corrosion current density in absence and presence of inhibitor, respectively.

3.3. Scanning electron microscopy (SEM)

The morphology of state surface was performed using a JEOL JSM-5800 Scanning Electron Microscopy. The energy of the acceleration beam employed was 20 kV. The analysis by SEM was carried out on the surface of carbon steel samples before and after immersion in the acidic solutions with and without the optimal concentration of PHQ inhibitor.

4. Quantum chemical calculations

Density Functional theory (DFT) has been recently used [42-45], to describe the interaction between the inhibitor molecule and the surface as well as the properties of these inhibitors concerning their reactivity. The molecular band gap was computed as the first vertical electronic excitation energy from the ground state using the time-dependent density functional theory (TD-DFT) approach as implemented in Gaussian 03[46]. For these seek, some molecular descriptors, such as HOMO and LUMO energy values, frontier orbital energy gap, molecular dipole moment, electronegativity (χ), global hardness (η), softness (σ), the fraction of electron transferred (ΔN), were calculated using the DFT method and have been used to understand the properties and activity of the newly prepared compounds and to help in the explanation of the experimental data obtained for the corrosion process.

According to Koopman's theorem [47], the ionization potential (IE) and electron affinity (EA) of the inhibitors are calculated using the following equations.

$IE = -E_{HOMO}$ (4)

$EA = -E_{LUMO}$ (5)

Thus, the values of the electronegativity (χ) and the chemical hardness (η) according to Pearson, operational and approximate definitions can be evaluated using the following relations [48]:

$$\chi = \frac{IE + EA}{2} \quad (6)$$

$$\eta = \frac{IE - EA}{2} \quad (7)$$

Global chemical softness (σ), which describes the capacity of an atom or group of atoms to receive electrons [43], was estimated by using the equation:

$$\sigma = \frac{1}{\eta} = -\frac{2}{E_{HOMO} - E_{LUMO}} \quad (8)$$

The number of transferred electrons (ΔN) was also calculated depending on the quantum chemical method [49, 50], by according the equation:

$$\Delta N = \frac{\chi_{Fe} - \chi_{inh}}{2(\eta_{Fe} + \eta_{inh})} \quad (9)$$

Where χ_{Fe} and χ_{inh} denote the absolute electronegativity of iron and inhibitor molecule η_{Fe} and η_{inh} denote the absolute hardness of iron and the inhibitor molecule respectively. In this study, we use the theoretical value of χ_{Fe} =7.0 eV and η_{Fe} = 0, for calculating the number of electron transferred.

5. RESULTS AND DISCUSSION

5. 1.Effect of PHQ concentration

5.1.1. Electrochemical impedance spectroscopy

The corrosion behaviour of carbon steel in acidic solution in the presence of PHQ was investigated by electrochemical impedance spectroscopy (EIS) at 303 K after 30 min of immersion at corrosion potential. Nyquist

plots of steel in inhibited and uninhibited acidic solutions containing various concentrations of PHQ are shown in Fig. 2. The impedance parameters derived from these plots are given in Table 1. Double layer capacitance values (C_{dl}) and charge-transfer resistance values (R_{ct}) were obtained from impedance measurements.
The double layer capacitance (C_{dl}) and the frequency at which the imaginary component of the impedance is maximal ($-Z_{max}$) are found as represented in equation 10:

$$C_{dl} = \left(\frac{1}{\omega R_t} \right) \qquad \text{Where} \qquad \omega = 2\pi f_{max} \tag{10}$$

The Nyquist plots for all PHQ concentrations are characterized by one semicircular capacitive loop. The presence of inhibitor introduces the diffusion step in corrosion process and the reaction becomes diffusion-controlled. Hence, the corrosion process can have two steps as in any electrochemical process at the electrochemical interface, first, the oxidation of the metal (charge transfer process) and second, the diffusion of the metallic ions from the metal surface to the solution (mass transport process). Inhibitor gets adsorbed on the electrode surface and thereby produces a barrier for the metal to diffuse out to the bulk and this barrier increases with increasing the inhibitor concentration [51]. The diameter of the semicircular capacitive loop (Fig. 2), the impedance of the double layer increased with increasing concentration of the PHQ. The general overview of the electrochemical impedance results meets the expectations from the theory of the technique, but it must be noted that the capacitive loops are depressed ones with centers under the real axis even though they have a semicircle appearance. Deviations of this kind are mostly referred to as frequency dispersion and they are attributed to irregularities and heterogeneities of the solid surfaces [52, 53]. In addition in the real corrosion systems, the double layer on the interface of metal/solution does not behave as a real capacitor. On the metal side of the double layer, the charge distribution is controlled by electron, whereas on the solution side it is controlled by ions [54].

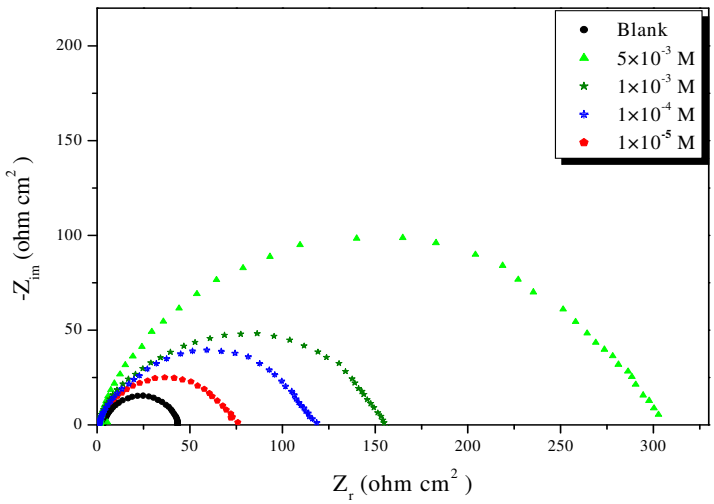

Figure 2: Nyquist diagrams for carbon steel in 1.0 M HCl containing different concentrations of PHQ at 303 K.

It is found (Table 1) that, as the PHQ concentration increases, the R_{ct} values increase, but the C_{dl} values tend to decrease. The decrease in C_{dl} values is interpreted by the adsorption of PHQ on the metal surface [55]. It is apparent from Nyquist diagrams that the charge-transfer resistance value of carbon steel in uninhibited 1.0 M HCl solution changes significantly after the addition of the inhibitor. Furthermore, C_{dl} decreases with increase of the concentration of inhibitor. This phenomenon is generally related to the adsorption of organic molecules on the metal surface and then leads to a decrease in the local dielectric constant and/or an increase in the thickness of the electrical double layer [56].

$$C_{dl} = \frac{\varepsilon_o \varepsilon}{\delta} S \tag{11}$$

Where δ is the thickness of the protective layer, S is the electrode area, ε_o the vacuum permittivity of vide and ε is dielectric constant of the medium.
A low capacitance may result if water molecules at the electrode interface are largely replaced by organic inhibitor molecules through adsorption [57]. The larger inhibitor molecules also reduce the capacitance through the increase in

the double layer thickness [58]. The inhibiting effectiveness increases with the concentration of the inhibitor to reach a maximum value from 86.1% to 5.10^{-3} M.

Table 1: Electrochemical impedance parameters and the corresponding inhibition efficiencies for carbon steel in 1.0 M HCl solution in the absence and presence of four different concentrations of PHQ

Inhibitor	Conc (M)	R_{ct} (Ω cm^2)	f_{max} (Hz)	C_{dl} (μF/cm^2)	η_z (%)
Blank	1.0	44.1	36.85	98	-----
PHQ	5×10^{-3}	300.1	12.34	43	86.1
	1×10^{-3}	163.5	20.29	48	73.0
	1×10^{-4}	114.1	29.69	47	63.3
	1×10^{-5}	79 .7	29.69	68	44.7

5.1.2. Tafel polarisation study

The potentiodynamic polarization curves for carbon steel in 1.0 M HCl solution after immersion time of 30 min in the absence and presence of various concentrations of PHQ are shown in Figure 3.

Polarization curves indicate that used inhibitor has inhibition effect on both cathodic and anodic reactions of the corrosion process. Therefore, this compound can be classified as mixed type inhibitor.

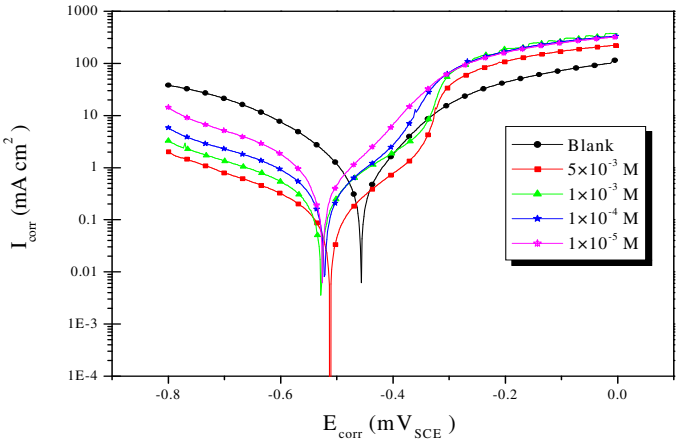

Figure 3: Typical polarization curves for carbon steel in 1.0 M HCl for various concentrations of PHQ at 303 K.

Electrochemical corrosion parameters such as corrosion potential (E_{corr}), cathodic Tafel slops (β_c) and corrosion current density (I_{corr}), obtained by extrapolation of Tafel lines, are collected in Table 2.

Table 2: Potentiodynamic electrochemical parameters for the corrosion of carbon steel in 1.0 M HCl solution in the absence and presence of PHQ at 303 K.

Inhibitor	Conc (M)	$-E_{corr}$ (mV_{SCE})	$-\beta_c$ (mV dec^{-1})	I_{corr} (μA cm^{-2})	η_{Tafel} (%)
Blank	1.0	459	102	455.5	-----
PHQ	5×10^{-3}	514	84	48.8	89.0
	1×10^{-3}	531	89	108.5	76.1
	1×10^{-4}	524	94	171.5	62.3
	1×10^{-5}	528	82	260.1	43.4

The obtained results show that the inhibition efficiency increased, while the corrosion current density decreased when the concentration of the inhibitor is increased. This could be explained on the basis of adsorption of PHQ on the carbon steel surface and the adsorption process enhanced with increasing inhibitor concentration. The data in Table 2 show that increasing PHQ concentration slightly shifts the values of corrosion potential (E_{corr}) in cathodic direction indicating that it acts as mixed-type inhibitor. The cathodic Tafel slope (β_c) show slight changes with the addition of

PHQ, which suggests that the inhibiting action occurred by simple blocking of the available cathodic sites on the metal surface, which lead to a decrease in the exposed area necessary for hydrogen evolution and lowered the dissolution rate with increasing PHQ concentration. The parallel cathodic Tafel plots obtained in Fig. 3 indicate that the hydrogen evolution is activation-controlled and the reduction mechanism is not affected by the presence of inhibitor [59].The inhibitory effectiveness of PHQ increases with concentration and reached a maximum value of about 89% to 5×10^{-3}M.

5.2. Effect of temperature

The effect of temperature on the inhibition performance of PHQ for carbon steel in 1.0 M HCl solution in the absence and presence of 5×10^{-3} M concentration at temperature ranging from 303 to 333 K was obtained by potentiodynamic polarization measurements (Figs 4 and 5). Corresponding data are given in Table 3. Inhibitory efficiency decreases with increasing temperature of 303-333 K in the presence and absence of PHQ, this behavior leads to the rise of the current density, this increase in temperature affects the bonds linking between inhibitor and the carbon steel surface. This result led to the dissolution or to the organic molecule or to the carbon steel.

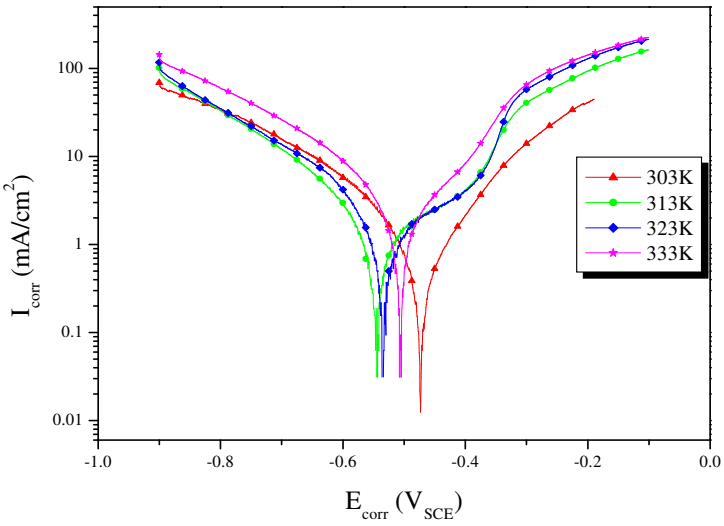

Figure 4: Potentiodynamic polarisation curves of carbon steel in 1.0 M HCl at different temperature

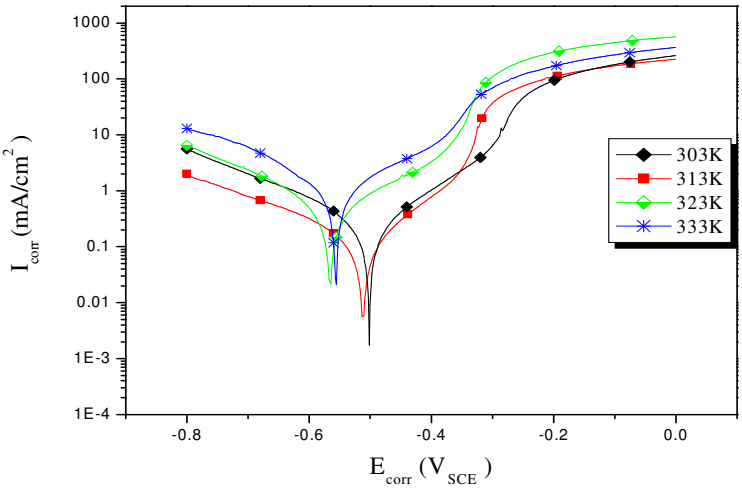

Figure 5: Potentiodynamic polarisation curves of carbon steel in 1.0 M HCl in the presence of the optimum concentration of PHQ at different temperatures.

Table 3: Electrochemical characteristics of carbon steel in 1.0 M HCl without and with 5×10^{-3}M of the studied inhibitor at different temperatures derived from current-voltage I-E characteristics.

Inhibitor	Temp (K)	$-E_{corr}$ (mV_{SCE})	$-\beta_c$ ($mV\ dec^{-1}$)	I_{corr} ($\mu A\ cm^{-2}$)	η_{Tafel} (%)
	303	459.4	102.0	455.5	----
	313	535.6	123.8	1020	----
Blank	323	545.6	143.3	1150	----
	333	507.0	149.3	1460	----
	303	514.4	83.8	48.8	89.0
PHQ	313	503.9	141.3	164.7	83.9
	323	568.3	161.0	390.4	66.0
	333	558.7	133.1	622.1	57.3

We were interested in the activation energy of the corrosion process and the kinetic parameters of the quinoxaline derivative adsorption. This was accomplished by investigating the temperature dependence of the corrosion current, obtained using Tafel extrapolation method. The corrosion reaction can be regarded as an Arrhenius-type process, the rate is given by:

$$I_{corr} = k \exp\left(-\frac{E_a}{RT}\right) \quad (12)$$

Where E_a is the apparent activation corrosion energy, T is the absolute temperature, A is the Arrhenius pre-exponential constant and R is the universal gas constant. This equation can be used to calculate the Ea values of the corrosion reaction without and with PHQ. The logarithm of the corrosion current density versus 1000/T and the activation energy (Ea) values can be calculated from the Arrhenius slope (Fig. 6). The calculated values of the apparent activation corrosion energy in the absence and presence of PHQ are listed in Table 4.

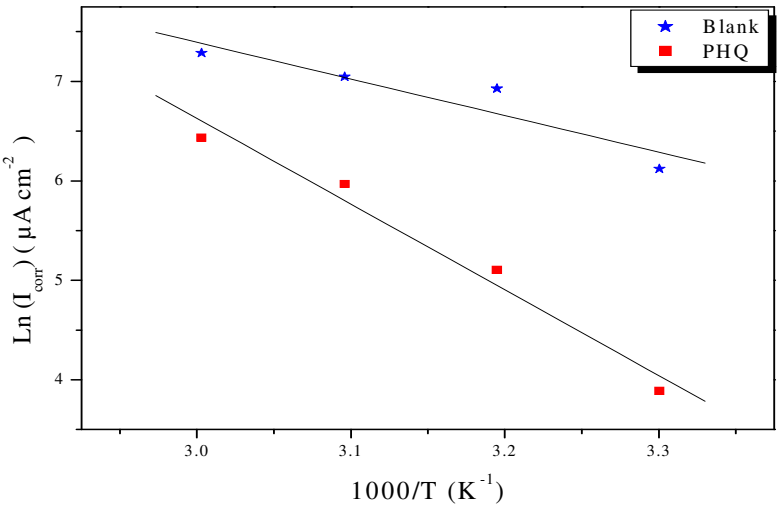

Figure 6: Arrhenius plots of carbon steel in 1.0 M HCl with and without 5×10^{-3} M of PHQ.

In 1.0 M HCl, the addition of quinoxaline derivative to an increase in the apparent activation energy to values greater than that of the uninhibited solution. Addition of PHQ in 1.0 M HCl increases the activation energy from 30.60 to 71.65 kJ/mol. It is clear that the activation energy increases with the addition of PHQ. Consequently, the rate of corrosion decreases due to the formation of the metal complex layer [60]. Szauer and Brand explained that the

increase in activation energy can be attributed to an appreciable decrease in the adsorption of the inhibitor on the carbon steel surface with the increase in temperature. When there is reduction in the adsorption, a greater desorption of the inhibitory molecules occurs because these two opposite processes are in equilibrium. Because of this most important desorption of the inhibitor molecules at higher temperatures, a greater carbon steel surface is in contact with aggressive environment, involving higher corrosion rates with increasing temperature [61].
An alternative formulation of Arrhenius equation is [62]:

$$I_{corr} = \frac{RT}{Nh}\exp\left(\frac{\Delta S_a}{R}\right)\exp\left(\frac{\Delta H_a}{RT}\right) \quad (13)$$

Where T the absolute temperature, h the Planck's constant, N the Avogadro's number, ΔS_a the entropy of activation, ΔH_a the enthalpy of activation and I_{corr} is the corrosion rate.
The plots of Ln (I_{corr}/T) versus 1000/T (Fig. 7) show almost straight lines and all the regression coefficients are close to 1. From the slopes and intercepts of the straight lines, the values of ΔH_a and ΔSa were calculated and listed in Table 4.

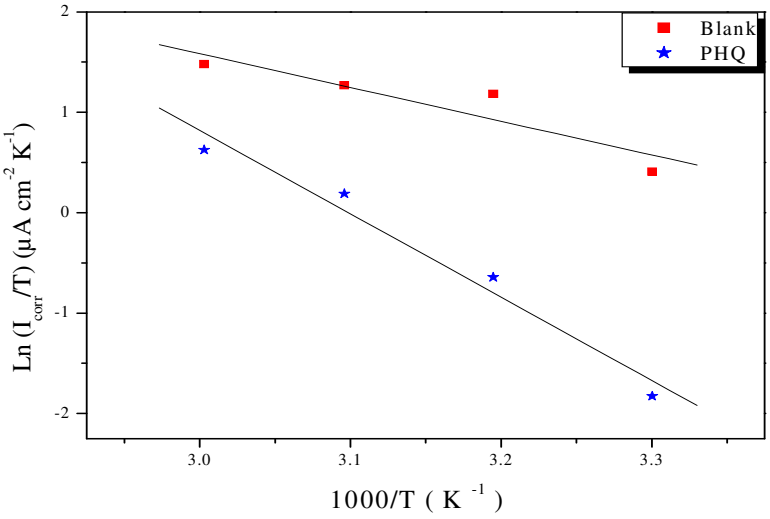

Figure 7: Transition state plots for carbon steel in 1.0 M HCl and 1.0 M HCl + 5 mM PHQ.

Table 4: The values of activation parameters for carbon steel in 1.0 M HCl in the absence and presence of 5 mM of PHQ

Conc (M)	E_a (kJ mol^{-1})	ΔH_a (kJ mol^{-1})	ΔS_a (J mol^{-1} K^{-1})
Blank	30.60	27.96	-23.89
PHQ	71.65	60.01	92.88

Examination of these data reveals that the ΔH_a value for dissolution reaction of carbon steel in 1.0 M HCl in the presence of PHQ are higher than that in the absence of PHQ, The positive sign of ΔHa show the endothermic nature of the solution process suggesting that the dissolution of carbon steel is slow [61].
In the absence of HQP for carbon steel the large negative value of a ΔS_a implies that the activated complex is the rate determining step, rather than the dissociation step. In the presence of the inhibitor, the values of a ΔS_a increases and is generally interpreted as an increase in disorder as the reactants are converted to the activated complexes, simply the disorder increases with PHQ [62-67].

5.3. Adsorption isotherm
Organic inhibitors exhibit inhibition ability via adsorption on the solution/metal interface, while the adsorption isotherm can provide the basic information about the interaction between the inhibitor and the metal surface [68,69].We tested various adsorption isotherms to fit the experimental data, such as Langmuir, Temkin, Flory-Huggins and Frumkin adsorption isotherms. For PHQ, the plot of C versus C/θ yield sastraight line with slope nearly

1 and the linear association coefficient (R^2) is also nearly 1 (Fig.8), showing that the adsorption of PHQ on the carbon steel surface can be well described by Langmuir adsorption isotherm: Eq.(14). This kind of isotherm involves the single layer adsorption characteristic and no interaction between the adsorbed inhibitor molecules on the carbon steel surface [70, 71].

$$\frac{C}{\theta} = \frac{1}{K_{ads}} + C \qquad (14)$$

Where Kads is the adsorption constant, C is the concentration of the inhibitor and surface coverage values (θ) are obtained according to the following equation:

$$\theta = \left(\eta_{Tafel}\%\right)/100 \qquad (15)$$

The constant of adsorption, K_{ads}, is related to the standard free energy of adsorption, ΔG°_{ads}, with the following equation:

$$\Delta G^{\circ}_{ads} = -RTLn\left(55.5K_{ads}\right) \qquad (16)$$

Where R is the universal gas constant, T is the thermodynamic temperature and the value of 55.5 is the concentration of water in the solution in mol/L.

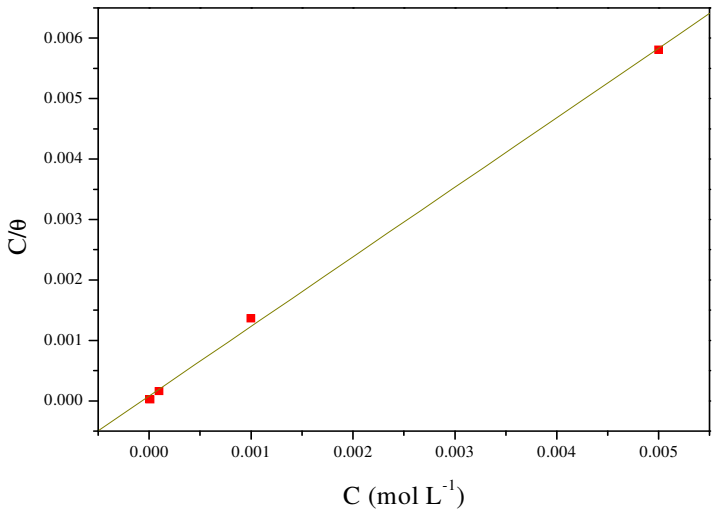

Figure 8: Langmuir adsorption of PHQ on the carbon steel surface in 1.0 M HCl solution.

The thermodynamic parameters for the adsorption process were obtained from this figure are shown in Table 5.

Table 5: Thermodynamic parameters for the adsorption of PHQ in 1.0 M HCl on the carbon steel at 303K.

	Slope	R^2	K_{ads} (L mol^{-1})	ΔG°_{ads} (KJ/mol)
PHQ	1.1	0.99949	12539.9	-33.90

The value of ΔG°_{ads} is negative which indicate that these investigated compound is strongly adsorbed on the carbon steel surface and show the spontaneity of the adsorption process and stability of the adsorbed layer on the carbon steel surface. Generally, values of ΔG°_{ads} up to -20 kJ mol-1 are consistent with the electrostatic interaction between the charged molecules and the charged metal (physical adsorption) while those more negative than -40 kJ mol-1 involve sharing or transfer of electrons from the inhibitor molecules to the metal surface to form a coordinate type of bond (chemisorption) [72]. It can be assumed that the adsorption of PHQ on mild steel surface occurs first due to electrostatic interaction, and then the desorption of water molecules is accompanied by chemical interaction between the adsorbate and metal surface [73].

5.4. SEM analysis

Scanning electron micrographs (Fig. 9) of the carbon steel surface before and after of the immersion in 1.0 M HCl with and without addition of PHQ were taken in order to establish whether inhibition is due to the formation of an organic film on the metal surface. Considering the result of the SEM studies on carbon steel before its immersion in the solution, except the presence of polishing scratches, the surface shows the absence of noticeable defects such as pits and cracks Fig 9a. Figs. 9b and 9c show the steel surface after 6 h of immersion in 1.0 M HCl without and with 5×10^{-3} M of PHQ. The resulting of the high resolution SEM micrograph (Fig. 9b) shows that the steel surface was strongly damaged in the absence of the PHQ with the increased number and depth of the pits. However, there are less pits and cracks observed in the micrographs in the presence of PHQ (Fig. 9c) which suggests a formation of protective film on steel surface which was responsible for the corrosion inhibition. Indeed, PHQ has a strong tendency to adhere to the steel surface and can be regarded as good inhibitor for steel corrosion in normal hydrochloric medium. The high inhibitive performance of this quinoxaline derivative suggests a strong bonding of the PHQ on the metal surface due to presence of lone pairs from heteroatom (nitrogen) and π-orbitals, blocking the active sites and therefore decreasing the corrosion rate.

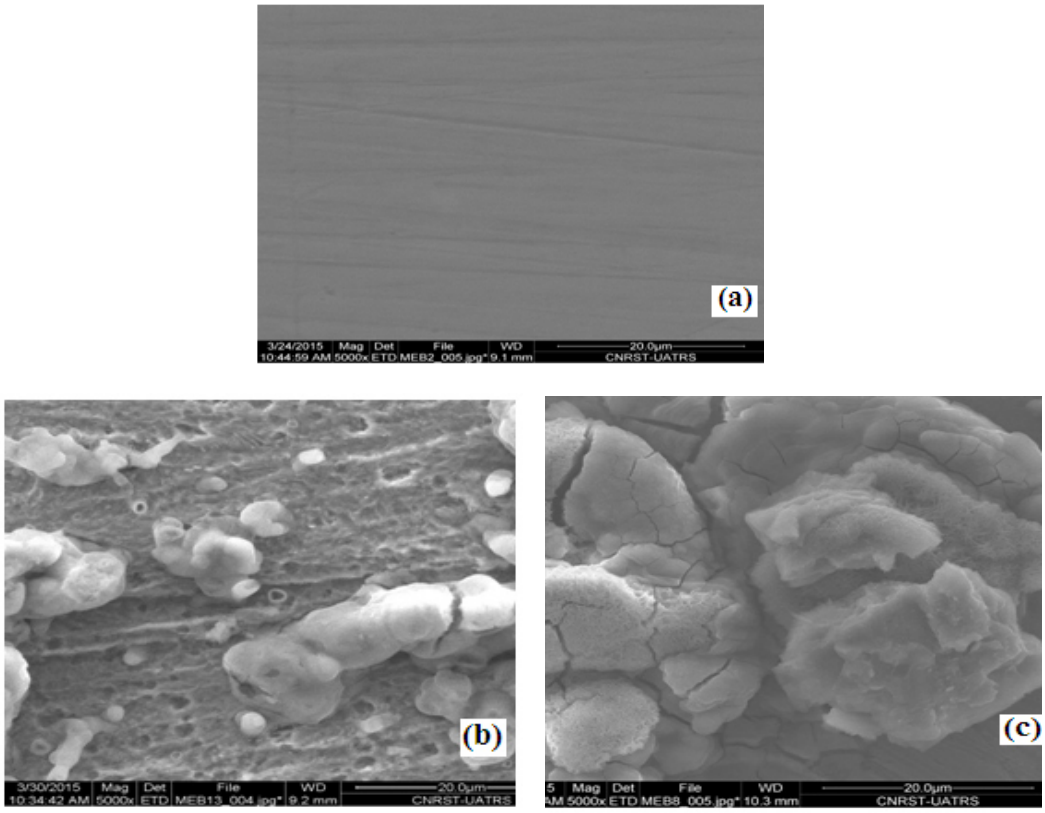

Figure 9: SEM micrographs of carbon steel samples at 303 K (a) only surface polishing, (b) after immersion in 1.0 M HCl without inhibitor, (c) after immersion in 1.0 M HCl in presence of 5×10^{-3} M PHQ.

6. Quantum chemical calculations

The experimental results provide evidence of the inhibition efficiency of the PHQ molecules, which may act through a chemical adsorption mechanism. To enhance the investigation of the electronic interaction between PHQ molecules and the carbon steel surface, several theoretical parameters, such as the molecular orbital energies (E_{HOMO}, E_{LUMO}),..., were determined by optimization. The quantum chemical parameters were the calculated ΔE, dipole moment, electronegativity (χ), global hardness (η), softness (σ) and the fraction of electron transferred (ΔN) [74,75]. To present detailed information, all of the results of the theoretical computations are reported (Table 6), and the optimized molecule structure (PHQ) is depicted in Fig.9.

The HOMO and LUMO diagrams (Fig. 9) of the inhibitor PHQ have reflected that the orbital electron densities were distributed homogeneously throughout the molecule. E_{HOMO} often is associated with the electron donating ability of the molecule. Higher values of E_{HOMO} are likely to indicate a tendency of the molecule to donate electrons to appropriate acceptor molecules to the unoccupied d orbital of a metal. It is well known that the electronic configuration of Fe atom is [Ar] $4s^2 3d^6$, and 3d orbital is not fully filled with electrons. The unfilled 3d orbital could bind with the HOMO of the inhibitors [76], whereas the filled 4s orbital could donate the electron to LUMO of the

inhibitors. So, it could be predicted that the adsorption of inhibitors on the carbon steel surface might be ascribed to the interaction between 3d, 4s orbitals of Fe atom and the front molecular orbitals of the inhibitor [77]. The energy of the lowest unoccupied molecular orbitals indicates the ability of the molecule to accept electrons.

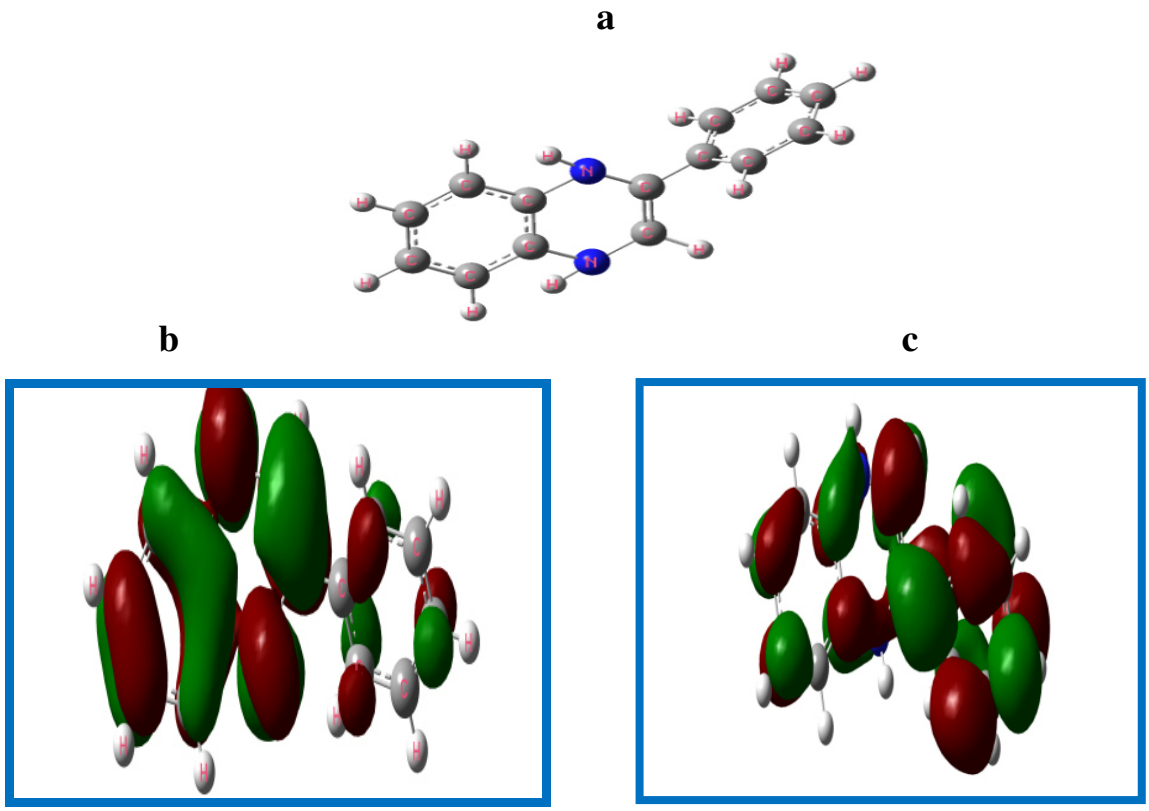

Figure 9: Optimized molecular structures of PHQ (a), HOMO (b) and LUMO (c) orbitals.

Table 6: Molecular properties of PHQ obtained from the optimized structure using DFT at the B3LYP/6-31G*.

Paramaters	PHQ
E_{HOMO} (eV)	-0.1588
E_{LUMO} (eV)	-0.0318
ΔE gap (eV)	0.1269
μ (debye)	1.4951
$I = -E_{HOMO}$ (eV)	0.1588
$A = -E_{LUMO}$ (eV)	0.0318
$\chi = \frac{I + A}{2}$ (eV)	0.0953
$\eta = \frac{I - A}{2}$ (eV)	0.0635
$\sigma = \frac{1}{\eta}$	15.748
$\Delta N = \frac{\chi_{Fe} - \chi_{inh}}{2(\eta_{Fe} + \eta_{inh})}$	0.5473
TE (eV)	-17689.29

The value of E_{LUMO} (-0.0318 eV) indicates its ability of the molecule to accept electrons. Therefore, the value of ΔE provides a measure for the stability of the formed complex on the metal surface. The high inhibition efficiency of a

molecule can be attributed to the high value of dipole moment and low value of ΔE. The results of the high dipole moment and the low energy gap indicate that electron transfer from PHQ to the surface takes place during adsorption to the carbon steel surface [78]. The total energy calculated by quantum chemical methods is equal to -17689.29 eV. Hohenberg and Kohn [79] proved that the total energy of a system including that of the many body effects of electrons (exchange and correlation) in the presence of static external potential (for example, the atomic nuclei) is a unique functional of the charge density. The minimum value of the total energy functional is the ground state energy of the system. The electronic charge density which yields this minimum is then the exact single particle ground state energy.
The values of χ, η, σ and ΔN are also listed in Table 6. According to some studies [80], the parameter of χ is related to the chemical potential, and higher value of χ means better inhibitive performance. On the other hand, η is equal to ΔE/2, and the lower c implies more polarizability and higher inhibition efficiency. The parameter of σ is reciprocal to η, thus high value of σ is related to more efficiency. Values of ΔN exhibit inhibitive performance resulted from electrons donations. If $\Delta N < 3.6$, the inhibition efficiency increases with the increase in electron-donation ability to the metal surface [80].

Conclusion

The PHQ is an efficient inhibitor for carbon steel in1.0 M HCl. The inhibition efficiency increases with the addition of inhibitor and reached a maximum of 89% in the presence of 5×10^{-3} M of inhibitor. The inhibition efficiency decreases with the increase in temperature. The adsorption of PHQ on carbon steel obeys Langmuir adsorption isotherm. The inhibitor retards both anodic and cathodic reactions on the surface of the metal. Thus, polarisation measurement suggests that the PHQ acts as a mixed type of inhibitor. The electrochemical impedance spectroscopy and SEM confirms the formation of protective film on the carbon steel surface.
Quantum chemical studies also support the experimental studies.

References

1. Strickland D.M., *Ind. Eng. Chem*. 15 (1923) 566.
2. Hatfield J.D., Slack, A.V., Crow, G.L., Shaffer, H.B., *J. Agric. Food Chem*. 6 (1958) 524.
3. Ji G., Shukla, S.K., Dwivedi, P., Sundaram, S., Prakash, R., *Ind. Eng. Chem. Res*. 50 (2011) 11954.
4. Singh A. K., Quraishi, M. A., *J. Mater. Environ. Sci.* 1 (2010) 101.
5. Prajila M., Sam, J., Bincy, J., Abraham, J., *J. Mater. Environ. Sci.* 3 (2012) 1045.
6. Naik U.J., Panchal, V.A., Patel, A.S., Shah, N.K., *J. Mater. Environ. Sci.* 3 (2012) 935.
7. Al Hamzi A.H., Zarrok, H., Zarrouk, A., Salghi, R., Hammouti, B., Al-Deyab, S.S., Bouachrine, M., Amine, A., Guenoun, F. *Int. J. Electrochem. Sci*. 8 (2013) 2586.
8. Zarrouk A., Hammouti, B., Zarrok, H., Warad, I., Bouachrine, M., *Der Pharm. Chem*. 3 (2011) 263.
9. Ben Hmamou D., Salghi, R., Zarrouk, A., Messali, M., Zarrok, H., Errami, M., Hammouti, B., Bazzi, L., Chakir A. *Der Pharm. Chem*. 4 (2012) 1496.
10. Ghazoui A., Bencaht, N., Al-Deyab, S.S., Zarrouk, A. , Hammouti, B., Ramdani, M., Guenbour, M. *Int. J. Electrochem. Sci*. 8 (2013) 2272.
11. Zarrouk A., Zarrok, H., Salghi, R., Bouroumane, N., Hammouti, B., Al-Deyab, S.S., Touzani, R. *Int. J. Electrochem. Sci*.7 (2012) 10215.
12. Bendaha H., Zarrouk, A., Aouniti, A., Hammouti, B., El Kadiri, S., Salghi, R., Touzani, R., *Phys. Chem. News* 64 (2012) 95.
13. Rekkab S., Zarrok, H., Salghi, R., Zarrouk, A., Bazzi, L., Hammouti, B., Kabouche, Z., Touzani, R., Zougagh M., *J. Mater. Environ. Sci.*3 (2012) 613.
14. Zarrouk A., Hammouti, B., Zarrok, H., Bouachrine, M., Khaled, K.F., Al-Deyab, S.S. *Int. J. Electrochem. Sci*.7 (2012) 89.
15. Ghazoui A., Saddik, R., Benchat, N., Guenbour, M., Hammouti, B., Al-Deyab, S.S., Zarrouk, A. *Int. J. Electrochem. Sci*.7 (2012) 7080.
16. Zarrok H., Mamari, K.A., Zarrouk, A., Salghi, R., Hammouti, B., Al-Deyab, S.S., Essassi, E.M., Bentiss, F., Oudda, H., *Int. J. Electrochem. Sci*. 7 (2012) 10338.
17. Zarrok H., Zarrouk, A., Salghi, R., Ramli, Y., Hammouti, B., Assouag, M., Essassi, E.M., Oudda, H., Taleb, M., *J. Chem. Pharm. Res*.4 (2012) 5048.
18. Zarrouk A., Hammouti, B., Dafali, A., Bentiss, F., *Ind. Eng. Chem. Res*. 52 (2013) 2560.

19. Zarrok H., Zarrouk, A., Salghi, R., Oudda, H., Hammouti, B., Assouag, M., Taleb, M., Ebn Touhami, M., Bouachrine M., Boukhris S., *J. Chem. Pharm. Res*. 4 (2012) 5056.
20. Zarrok H., Oudda H., El Midaoui, A., Zarrouk, A., Hammouti, B., Ebn Touhami, M., Attayibat, A. , Radi, S., Touzani R., *Res. Chem. Intermed*. 38 (2012) 2051.
21. Ghazoui A., Zarrouk, A., Bencaht, N., Salghi, R., Assouag, M., El Hezzat, M., Guenbour, A., Hammouti, B., *J. Chem. Pharm. Res*.6 (2014) 704.
22. Zarrok H., Zarrouk A., Salghi, R., Ebn Touhami, M., Oudda, H., Hammouti, B., Touir, R., Bentiss, F., Al-Deyab S.S., *Int. J. Electrochem. Sci*. 8 (2013) 6014.
23. Zarrouk, A., Zarrok, H., Salghi, R., Touir, R., Hammouti, B., Benchat, N., Afrine, L.L., Hannache, H., El Hezzat, M., Bouachrine, M., *J. Chem. Pharm. Res*.5 (2013) 1482.
24. Zarrok H., Zarrouk, A., Salghi, R., Assouag, M., Hammouti, B., Oudda, H., Boukhris, S., Al Deyab, S.S., Warad I., *Der Pharm. Lett.* 5 (2013) 43.
25. Ben Hmamou D., Aouad, M.R., Salghi, R., Zarrouk, A., Assouag, M., Benali, O., Messali, M., Zarrok, H., Hammouti B., *J. Chem. Pharm. Res*. 4 (2012) 3498.
26. Bailly C., Waring M.J., *J. Biochem*. 330 (1998) 81.
27. Addess K.J., Feigon, J., *Nucleic Acids Res*. 22 (1994) 54845.
28. Branka J.E., Vallette, G., Jarry, A., Laboisse, C.L., *J. Biochem*. 323 (1997) 521.
29. Stilwell W.G., Turesky, R.J., Sinha, R., Skiper, P.L., Tannenbaum, S.R., *Cancer Lett*. 143 (1999) 145.
30. Tayebi H. Bourazmi, H. Himmi, B. El Assyry, A. Ramli, Y. Zarrouk, A. Geunbour, A. Hammouti, B., *Der Pharm. Chem*. 6 (5) (2014) 220.
31. Bahri S., Belayachi, M., Zarok, H., Shaim, A., Galai, M., Zarrouk, A., El Midaoui, A., Ebn Touhami, M., Lakhrissi B., Oudda, H., *Der Pharm. Chem*. 6 (3) (2014) 110.
32. Adardour K., Touir, R., Elbakri, M., Ramli, Y., Ebn Touhami, M., El Kafsaoui, H., Mubengayi, C.K., Essassi E.M., *Res.Chem. Intermed.* 39 (9) (2013) 4175.
33. Zarrok H., Zarrouk, A., Salghi, R., Elmahi, B., Hammouti, B., Al-Deyab, S.S., Ebn Touhami, M., Bouachrine M., Oudda, H., Boukhris, S., *Int. J. Electrochem. Sci*. 8 (9) (2013) 11474.
34. Adardour K., Touir R., El bakri M., Larhzil, H., Ebn Touhami, M., Ramli, Y., Zarrouk, A., El Kafsaoui, H., Essassi E.M., *Res.Chem. Intermed*. (2013) 1.
35. Fu J., Zang, H., Wang, Y., Li, S., Chen, T., Liu, X., *Ind. Eng. Chem. Res*. 51 (18) (2012) 6377.
36. Etaiw S.E.D.H., Fouda, A.E.A.S., Abdou, S.N., El-bendary, M.M., *Corros. Sci*. 53 (11) (2011) 3657.
37. Chitra S., Parameswari, K., Vidhya, M., Kalishwari, M., Selvaraj, A., *Int. J. Electrochem. Sci*. 6 (10) (2011) 4593.
38. Doner A., Solmaz, R., Ozcan, M., Kardas, G., *Corros. Sci.* 53 (2011) 2902.
39. Obot I.B., Gasem, Z.M., *Corros. Sci.* 83 (2014) 359.
40. Zarrok H., Zarrouk, A., Salghi, R., Oudda, H., Hammouti, B., Ebn Touhami, M., Bouachrine, M., Pucci, O.H., *Port. Electrochim. Acta* 30 (2012) 405.
41. Belayachi M., Serrar, H., Zarrok, H., El Assyry, A., Zarrouk, A., Oudda, H., Boukhris, S., Hammouti, B., Ebenso Eno E., Geunbour, A., *Int. J. Electrochem. Sci.,* 10 (2015) 3010.
42. Ma H., Chen, S., Liu, Z., Sun, Y., J. Mol. Struct., (THEOCHEM) 774 (2006) 19.
43. Henríquez-Román J.H., Padilla-Campos, L., Páez, M.A., Zagal, J.H., María Rubio, A., Rangel, C.M., Costamagna J., Cárdenas-Jirón, G., *J. Mol. Struct., (THEOCHEM)* 757 (2005) 1.
44. Rodrguez-Valdez L.M., Martnez-Villafane, A., Glossman-Mitnik, D., *J. Mol. Struct. (THEOCHEM)* 713 (2005) 6.
45. Feng Y., Chen, S., Guo, W., Zhang, Y., Liu, G., *J. Electroanal. Chem*., *602* (2007) 115.
46. Frisch M.J., Trucks, G.W., Schlegel, H.B., Scuseria, G.E., Robb, M.A., Cheeseman, J.R., Montgomery, J.A.Jr., Vreven, T., Kudin, K.N., Burant, J.C., Millam, J.M., Iyengar, S.S., Tomasi, J., Barone, V., Mennucci, B., Cossi, M., Scalmani, G., Rega, N., Petersson, G.A., Nakatsuji, H.,Hada, M., Ehara, M., Toyota, K., Fukuda, R., Hasegawa, J., Ishida, M., Nakajima, T., Honda, Y., Kitao, O., Nakai, H., Klene, M., Li, X., Knox, J.E., Hratchian, H.P., Cross, J.B., Bakken, V., Adamo, C., Jaramillo, J., Gomperts, R., Stratmann, R.E., Yazyev, O., Austin, A.J., Cammi, R., Pomelli, C., Ochterski, J.W., Ayala, P.Y., Morokuma, K., Voth, G.A., Salvador, P., Dannenberg, J.J., Zakrzewski, V.G., Dapprich S., Daniels, A.D., Strain, M.C., Farkas, O., Malick, D.K., Rabuck, A.D., Raghavachari, K., Foresman, J.B., Ortiz, J.V., Cui, Q., Baboul, A.G., Clifford, S., Cioslowski, J., Stefanov, B.B., Liu, G., Liashenko, A., Piskorz, P., Komaromi, I.; Martin, R.L.; Fox, D.J.; Keith, T.; Al-Laham, M.A.; Peng, C.Y.; Nanayakkara, A.; Challacombe, M., Gill, P.M.W., Johnson, B.,

Chen W., Wong M.W., Gonzalez C., Pople J.A., *Gaussian 03, Revision E.01, Gaussian, Inc., Wallingford CT*, 2004.
47. Dewar M.J.S., Thiel W., *J. Am. Chem. Soc*., 99 (1977) 4899.
48. Pearson R.G., *Inorg. Chem*., 27 (1988) 734.
49. Sastri V.S., Perumareddi, J.R., *Corrosion (NACE)* 53 (1997) 617.
50. Lukovits I., Kalman, E., Zucchi, F., *Corrosion(NACE)* 57 (2001) 3.
51. Satpati A.K., *Mater. Chem. Phys*. 109(2008)352.
52. Ozcan M., *J. Solid. State. Electrochem.* 12 (2008) 1653.
53. Juttner K., *Electrochim. Acta* 35 (1990) 1501.
54. Ozcan M., Dehri I., Erbil, M., *Appl. Surf. Sci.* 236(2004) 155.
55. Bentiss F., Lagrenee M., Traisnel M., Hornez J. C., *Corros. Sci.* 41 (1999) 89.
56. McCafferty E., Hackerman, N., *J. Electrochem. Soc.* 119 (1972) 146.
57. Li P., Lin J. Y., Tan K. L., Lee J. Y., *Electrochim Acta* 42 (1997) 605.
58. Abdel Rehim S. S., Hazzazi O. A., Amin M. A., Khaled K. F., *Corros. Sci.* 50 (2008) 2258.
59. Bentiss F., Jama, C., Mernari, B., El Attari, H., El Kadi, L., Lebrini, M., Traisnel M., Lagrenée M., *Corros. Sci.* 51 (2009) 1628.
60. Elaoufir Y., Bourazmi, H., Serrar, H., Zarrok, H., Zarrouk, A., Hammouti, B., Guenbour, A., Boukhriss, S., Oudda, H. *Der Pharm. Lett.* 6 (2014) 526.
61. Szauer T., Brand, A., *Electrochim. Acta* 26 (1981) 1253.
62. Guan N.M., Xueming, L., Fei, L., *Mater. Chem. Phys.* 86 (2004) 59.
63. El Ouali I., Hammouti, B., Aouniti, A., Ramli, Y., Azougagh, M., Essassi, E. M., Bouachrine, M., *J. Mater. Envir. Sci.* 1 (2010) 1.
64. Khamis E., Hosney, A., El-Khodary, S., Afinidad 52 (1995) 95.
65. Sahin M., Bilgic, S., Yilmaz, H., *Appl. Surf. Sci.* 195 (2002) 1.
66. Bayol E., Kayakırılmaz, K., Erbil, M., *Mater. Chem. Phys.* 104 (2007) 74.
67. Ali S.A., Saeed, M.T., Rahman, S.U., *Corros. Sci.* 45 (2003) 253.
68. Zheng X.W., Zhang S.T., Li W.P., Yin L.L., He J.H., Wu J.F., *Corros. Sci*. 80 (2014) 383.
69. Musa A.Y., Kadhum A.A.H., Mohamad A.B., Takriff M.S., *Corros. Sci.* 52 (2010) 3331.
70. Outirite M., Lagrenée M., Lebrini M., Traisnel M., Jama C., Vezin H., Electrochim. Acta 55 (2010) 1670.
71. Elayyachy M., Idrissi A. E., Hammouti B., *Corros. Sci.* 48 (2006) 2470.
72. Bensajjay F., Alehyen, S., El-Achouri ,M. S., Kertit,S., *Anti-Corros. Methods Mater*. 50 (*2003)* 402.
73. Xu B., Liu, Y., Yin ,X.S., Yang, W.Z., Chen, Y. Z., *Corros. Sci*. 74 (2013) 206.
74. Herrag L., Hammouti B., Elkadiri S., Aouniti A., Jama C., Vezin H., Bentiss F., *Corros. Sci.* 52 (2010) 3042.
75. Deng S., Li X., Xie Xi., *Corros. Sci.* 80 (2014) 276.
76. Zhao P., Li Y., Liang Q., *Appl. Surf. Sci.* 252 (2005) 1596.
77. Ju H., Kai Z., Li Y., *Corros. Sci.* 50 (2008) 865.
78. Hong S., Chen W., Luo H.Q., Li N.B., *Corros. Science* 57 (2012) 270.
79. Rauk A., Orbital interaction Theory of Organic Chemistry, 2nd Edn (*John Wiley & Sons*: Newyork. (2001) 34.
80. Rodriguez L.M., Villamisr W., Martinez L., *Corros. Sci*. 48 (2006) 4053.